13th International Conference on Applications of Statistics and Probability in Civil Engineering, ICASP13
Seoul, South Korea, May 26-30, 2019

Experiments and FEA based Safety Factor Calibration for SFRRAC Beams

Rakul Bharatwaj Ramesh
Ph.D. student, Centre for Infrastructure Engineering, Western Sydney University, Penrith, Australia

Won-Hee Kang
Senior Lecturer, Centre for Infrastructure Engineering, Western Sydney University, Penrith, Australia

Olivia Mirza
Senior Lecturer, School of Computing, Engineering and Mathematics, Western Sydney University, Penrith, Australia

ABSTRACT: The objective of this research is to predict the design resistance of steel fibre reinforced recycled aggregate concrete (SFRRAC) beams using a statistical and probabilistic method. SFRRAC is a combination of recycled aggregate concrete (RAC) and steel fibres (SF). It is a sustainable and feasible alternative to natural aggregate concrete (NAC). Because existing structural design standards only provide design equations for NAC members, new design equations and corresponding capacity factors for SFRRAC members need to be developed. In this study, design resistance of SFRRAC beams is estimated based on a proposed resistance prediction model and an associated capacity factor. The capacity factor is calibrated based on the method provided in Eurocode 0 and the target reliability index given in ISO 2394:1998. However, the method is significantly modified to incorporate both experimental data and finite element analysis (FEA) results to estimate the model error of the resistance prediction model. The calibration utilizes recent flexural failure test data for 10 SFRRAC beams together with FEA results. Combining FEA results and experimental data increases the total number of data points and reduces the uncertainty due to a finite number of samples. However, at the same time, the inclusion of FEA results also adds their model uncertainties. The proposed method systematically selects the optimal number of FEA results to be combined with experimental data by considering the optimal balance between the reduced uncertainty due to the FEA data point addition and the increased uncertainty from FEA's model uncertainties.

1. INTRODUCTION

As the construction industry is rapidly growing, the importance given to sustainable construction techniques has increased, to protect the environment and the limited reserves of natural resources. In order to reduce the negative environmental impact of the construction industry and to meet the increasing global demand for raw materials, the significance of recycling and reusing construction waste has increased over the years. Considering the wide applications of concrete and the large consumption of coarse aggregates used in concrete on a global scale, using Recycled Aggregate (RA) in concrete is an environment-friendly and sustainable construction alternative.

However, Recycled Aggregate Concrete (RAC) does not exhibit adequate structural performance due to its inferior material properties compared to those of Natural Aggregate Concrete (NAC) (Ravindrarajah, 1996; Schubert et al., 2012). At present, RAC is restricted to limited structural use and is extensively used only in pavements and as shotcrete in tunnels. In this study, Steel Fibre (SF) is added to RAC to improve its structural performance. SF improves the mechanical performance of RAC and makes it suitable for

structural applications, especially under flexural load (Zhang and Pei, 2017; Salman and Abdul-Ameer, 2018). This research aims to replace NAC with RAC that incorporates SF. The use of the new material, Steel Fibre Reinforced Recycled Aggregate Concrete (SFRRAC), in fabricating structural members subjected to flexure is proposed to gain advantages in terms of environmental effects, production costs and structural properties.

Structural members fabricated using a new material such as SFRRAC should be designed according to proper design models and guidelines. The current design guidelines are limited to NAC and cannot be directly applied to SFRRAC due to the change in the material properties. This study estimates the design resistance of SFRRAC beams based on a proposed theoretical model that predicts the moment-capacity of SFRRAC beam cross-sections, which is presented in Section 2 of this paper, and the associated capacity factor.

The capacity factor is calibrated based on the calibration method provided in Eurocode 0 (BSI, 2002), which is modified in this study to incorporate both experimental data and finite element analysis (FEA) results. The experimental and FEA data used in this study are presented in Section 3, while the capacity factor calibration is presented in Section 4.

2. PROPOSED MOMENT-CAPACITY PREDICTION MODEL FOR SFRRAC CROSS-SECTIONS

This section proposes a prediction model for the flexural resistance of SFRRAC beams by considering the effect of SF. The current structural design codes AS 3600 (Standards Australia, 2009), ACI 318-11 (ACI, 2011) and Eurocode 2 (BSI, 2004) do not provide a prediction model to represent the effect of SF added to RC beams. To calculate the flexural resistance of SFRRAC beams, it is important to know the following: (i) the stress-strain relation of concrete and (ii) how to add the effect of SF. Figure 1 shows the stress-strain diagram of a NAC beam without SF (Bandyopadhyay, 2008). The depth of the neutral axis is denoted by x_{NA}. The effective depths of the steel reinforcement in the compression and tension zones are represented by d' and d, respectively. The ultimate strain in concrete is denoted by ε_{cu}. ε_{cs} and ε_s represent the strains in the compression reinforcement and tension reinforcement, respectively. The characteristic compressive strength of concrete and the yield strength of steel are denoted by f_c' and f_{sy}, respectively. The stress-block parameters γ and a represent the strength factor applied to concrete and the depth of the stress-block, respectively.

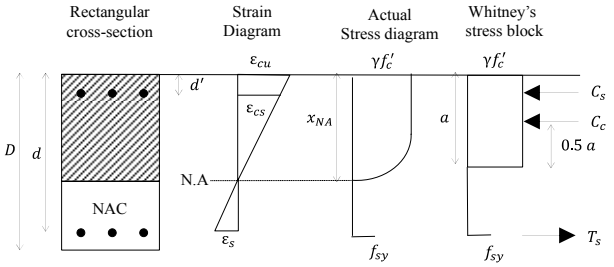

Figure 1: Stress and strain diagrams of doubly reinforced concrete (NAC) beam with rectangular cross-section

The Linear Bending Theory of steel reinforced concrete beams that is based on Hooke's Law neglects all the tensile stresses of concrete after the cracking of the cross-section. Hence, the concrete part below the neutral axis in a rectangular cross-section (the unshaded region in Figure 1) is disregarded in strength and moment-capacity calculations (Bandyopadhyay, 2008). In Figure 1, the compressive force in concrete (C_c) acts at a depth of 0.5 a from the top of the cross-section, and the compressive force in the compression reinforcement (C_s) acts at a depth of d' from the top. These forces are balanced by the tensile force in the tension reinforcement (T_s), which acts at the depth of d from the top.

In SFRRAC, the added SF improves the tensile strength of the concrete matrix. The horizontally striped region below the neutral axis in Figure 2 represents the contribution of SFRRAC to the tensile strength of the beam. In addition to the forces shown in Figure 1, a tensile force representing the tensile strength of

SFRRAC (T_{SFRRAC}) acts at a height of $(D - x_{NA})/2$ from the bottom as shown in Figure 2.

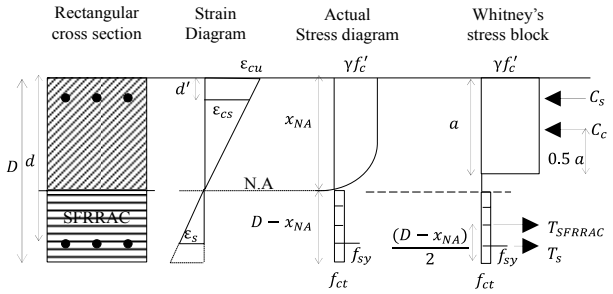

Figure 2: Stress and strain diagrams of doubly reinforced concrete (SFRRAC) beam with rectangular cross-section

3. EXPERIMENTAL RESULTS AND FINITE ELEMENT ANALYSIS RESULTS USED IN THE CAPACITY FACTOR CALIBRATION

In the experimental phase of this study, ten full-scale SFRRAC beams were cast and tested for flexural performance under three-point bending. While casting the SFRRAC beams, the raw materials such as cement, water, fine aggregate and coarse aggregate were added in the proportions of 717: 286: 420: 1011 kg/m^3. In addition, SF was added at a dosage of 0.7% by volume of concrete. Figure 3 shows the schematic diagram of the SFRRAC beams. The geometric dimensions of the beams tested and their moment-carrying capacities are presented in Table 1.

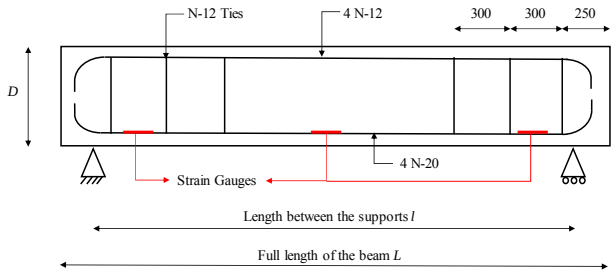

Figure 3: Schematic diagram of the beams

Table 1: Dimensions of SFRRAC beams experimentally tested in this study

Beam No.	Width (mm)	Depth (mm)	Length (mm)	Length between supports (mm)
1	300	400	3000	2600
2	340	450	3000	2600
3	375	500	3000	2600
4	450	600	3000	2600
5	300	400	3500	3100
6	300	400	4000	3600
7	300	400	4500	4100
8	300	400	5000	4600
9	300	400	2000	1600
10	300	400	2500	2100

In addition to the test results, FEA results of SFRRAC beams was also used in the capacity factor calibration in this study. A parametric study was adopted in FEA, in which the length of the SFRRAC beam models was varied between 2000 mm to 5000 mm, and the cross-sectional size was varied between the smallest size (300 mm × 400 mm) and the largest size (600 mm × 600 mm) considered as shown in Table 2. The FE beam models were analyses for flexural capacity under three-point loading. The moment-capacity results obtained from such numerical simulations were used as additional data to expand the original experimental database consisting of 10 data.

Table 2: Dimensions of the SFRRAC beams analyzed in FEA

Beam No.	Width (mm)	Depth (mm)	Length (mm)	Length between supports (mm)
1	300	400	3000	2600
2	340	450	3000	2600
3	375	500	3000	2600
4	450	600	3000	2600
5	300	400	3500	3100
6	300	400	4000	3600
7	300	400	4500	4100

8	300	400	5000	4600
9	300	400	2000	1600
10	300	400	2500	2100

4. CAPACITY FACTOR CALIBRATION

The reliability analysis method provided in Annex D of Eurocode 0 (BSI, 2002) is used in this study to calibrate capacity factors for SFRRAC under flexure. This method, presented in Section 4.1 has provisions for using only experimental data. However, to relieve the conservatism embedded in the calibrated capacity factor due to the finite number of experimental data available, FEA results were added to the experimental database used in this study. Because the FEA results are not exactly equivalent to the experimental data as they have additional numerical error, the error was estimated and incorporated into the capacity factor calibration procedure provided in Eurocode 0 (BSI, 2002), as presented in Section 4.2.

4.1. Reliability analysis method provided in Eurocode 0 (BSI, 2002)

This study adopts a target reliability index of 3.8, which corresponds to the reliability class RC2 for a 50-year reference period (BSI, 2002; ISO, 1998). This target reliability index is paired with a log-normally distributed resistance and a normally distributed load. The load factor α_E and resistance factor α_R are taken as -0.7 and 0.8, respectively according to Annex C of Eurocode 0 (BSI, 2002). The numerical value of the target reliability index (β_t) adopted for material resistance in this study is $\alpha_R \times 3.8 = 0.8 \times 3.8 = 3.04$. The capacity factor for the ultimate moment-capacity of each beam (ϕ_i) is calculated using the following equation.

$$\phi_i = \frac{r_{di}}{r_{ki}} \quad (1)$$

where r_{di} and r_{ki} are the design and the characteristic capacity of the i^{th} beam, respectively and they are explained in Sections 4.1.1 and 4.1.2, respectively.

4.1.1. Calculation of design capacity

The following equation represents the formula used to calculate the design capacity of the i^{th} beam r_{di}:

$$r_{di} = \overline{b} \times r_{ti} \times \exp(-k_i \times Q_i - 0.5 \times Q_i^2) \quad (2)$$

where r_{ti} is the theoretical moment carrying capacity of the i^{th} beam (estimated using the proposed moment-capacity prediction method); $\overline{b}$ is the bias correction factor; k_i is the combined fractile factor of the i^{th} beam that accounts for the combined error due to the modelling error of the theoretical prediction model, the total parametric uncertainty in all the design parameters and the error due to the finite number of data used; and Q_i is a coefficient. The ratio of the experimentally measured beam capacity (r_e) and the theoretically predicted capacity (r_t) is modelled as a lognormal random variable. The mean of this lognormal random variable is represented by the bias correction factor $\overline{b}$, as shown in the following equation.

$$\overline{b} = \frac{\sum_i^n r_{ei} \times r_{ti}}{\sum_i^n r_{ti}^2} \quad (3)$$

where r_{ei} is the experimentally obtained moment carrying capacity of the i^{th} beam; and r_{ti} is the theoretical moment carrying capacity of the i^{th} beam. The prediction error or the modelling error in the proposed moment-capacity prediction method for the i^{th} beam can be calculated as follows:

$$\delta_i = \frac{r_{ei}}{\overline{b} r_{ti}} \quad (4)$$

where δ_i is the prediction error for the i^{th} beam; $\overline{b}$ is the bias correction factor; r_{ei} is the moment carrying capacity of the i^{th} beam obtained experimentally; r_{ti} is the moment carrying capacity of the i^{th} beam. The c.o.v. of the modelling error of the theoretical capacity prediction method is denoted by V_δ, and it is calculated by taking the statistical coefficient of variation (c.o.v.) of $\delta_1, \delta_2, \ldots, \delta_{10}$ (the prediction errors for each of the 10 SFRRAC beams), which are calculated using Equation 4. To account for the error due to the finite number of experimental

data used, the design fractile factor k_d is used in the calculation of the combined fractile factor of the i^{th} beam as shown by the following equation.

$$k_i = \frac{(k_d \times V_\delta^2 + \beta_t \times V_{rti}^2)}{V_{ri}^2} \quad (5)$$

where k_d is the design fractile factor corresponding to n (the number of test data) obtained from Annex D of Eurocode 0 (BSI, 2002); β_t = 3.04 is the target reliability index; V_{rti} is the c.o.v. of the total parametric uncertainty in the i^{th} beam and accounts for the uncertainty of all the parameters used (e.g., compressive strength of concrete, yield strength of steel, member dimensions); V_δ is the c.o.v. of the modelling error of the theoretical capacity prediction method; and V_{rti} is the c.o.v. of the combined modelling and parametric uncertainty in the i^{th} beam. The coefficient Q_i used in Equation 2 is calculated using the following equation.

$$Q_i = \sqrt{ln(1 + V_{ri}^2)} \quad (6)$$

where V_{ri} represents the c.o.v. of the combined modelling and parametric uncertainty in the i^{th} beam.

4.1.2 Calculation of characteristic capacity

The characteristic moment-capacity value r_{ki} for the i^{th} beam can alternatively be used when the nominal design moment-capacity value r_{ni} is not available. The characteristic moment-capacity r_{ki} is calculated by entering the characteristic values of material strengths, in the capacity prediction method. The following equations represent the characteristic values of the compressive strength of concrete (f'_{cki}) and the yield strength of the steel reinforcement bars (f_{syki}), respectively in the i^{th} beam, at 5% significance.

$$f'_{cki} = f'_{c_i} \times \exp(-k_n \times \sigma_{lnf'_{c_i}} - 0.5 \times \sigma^2_{lnf'_{c_i}}) \quad (7)$$

$$f_{syki} = f_{syni} \times \exp(-k_n \times \sigma_{lnf_{syi}} - 0.5 \times \sigma^2_{lnf_{syi}}) \quad (8)$$

where f'_{cki} is the characteristic value of concrete's compressive strength at 5% significance for the i^{th} beam, f'_{c_i} is the nominal value of the concrete's compressive strength for the i^{th} beam, and $\sigma_{lnf'_{c_i}}$ = 0.15 is the coefficient of variation (c.o.v.) of the concrete's compressive strength (Johnson and Huang, 1994), f_{syki} is the characteristic value of the steel reinforcement bar's yield strength at 5% significance for the i^{th} beam, f_{syi} is the nominal value of the steel reinforcement bar's yield strength for the i^{th} beam, $\sigma_{lnf_{syi}}$ = 0.07 is the c.o.v. of the steel reinforcement bar's yield strength (JCSS, 2001). The characteristic fractile factor (k_n) at 5% significance is 1.64 and obtained from Annex D of Eurocode 0 (BSI, 2002).

4.1.2 The new reliability analysis method proposed in this study to include FEA data

This study proposes a calibration method to estimate the capacity factor for SFRRAC under flexure using the combined database of experimental and FEA data. Since the FEA results are used in combination with experimental data, the modelling error of the FEA needs to also be taken into account while using the reliability analysis framework; this is explained in Section 4.1.2.1. Section 4.1.2.2 explains how the capacity factor is estimated using the proposed iterative procedure that step wisely adds FEA results. The calibrated capacity factor is discussed in Section 4.1.2.3.

4.1.2.1 Inclusion of the modelling error of FEA

First, FE models of the 10 experimental beams were compared with their experimental results to measure the uncertainties of the FEA results. The ratio of the experimentally measured moment-capacity (r_e) and the moment-capacity from FEA (r_{FEA}) was modelled as a lognormal random variable. The mean of this lognormal random variable is represented by the bias correction factor $\overline{b}_{FEA}$, as shown in the following equation:

$$\overline{b}_{FEA} = \frac{\sum_i^n r_{ei} \times r_{FEAi}}{\sum_i^n r_{FEAi}^2} \quad (9)$$

where r_{ei} is the experimentally obtained moment carrying capacity of the i^{th} beam; and r_{FEAi} is the moment-carrying capacity of the i^{th} beam from

FEA. Second, the prediction error between the moment-capacity obtained from FEA and the experimental moment-capacity for the i^{th} beam is calculated as follows:

$$\delta_{FEAi} = \frac{r_{ei}}{\overline{b}_{FEA} \times r_{FEAi}} \quad (10)$$

where δ_{FEAi} is the prediction error between FEA and experiment for the i^{th} beam; $\overline{b}_{FEA}$ is the bias correction factor for the FEA results with respect to the experimental data; r_{ei} is the moment carrying capacity of the i^{th} beam obtained experimentally; r_{FEAi} is the moment carrying capacity of the i^{th} beam from FEA. The c.o.v. of the modelling error of FEA in predicting the moment-capacities of the 10 experimental beams (V_{FEA}) is calculated to be the statistical coefficient of variation (c.o.v.) of $\delta_{FEA1}, \delta_{FEA2}, \dots, \delta_{FEA10}$. To rigorously account for the error due to the finite number of experimental data used to validate the accuracy of the FEA, the following equation that includes the design fractile factor k_{dFEA} should used to find k_i.

$$k_i = \frac{(k_d \times V_\delta^2 + \beta_t \times V_{rti}^2 + k_{dFEA} \times V_{FEA}^2)}{V_\delta^2 + V_{rti}^2 + V_{FEA}^2} \quad (11)$$

where k_{dFEA} is the fractile factor corresponding to n_{FEA} = 10, the number of experimental data used to validate the accuracy of the FEA.

4.1.2.2 The proposed iterative procedure to find the capacity factor

An iterative procedure is proposed to find the required number of FEA results to be added to the experimental database to estimate a converged capacity factor for SFRRAC under flexure. In the first iteration, capacity factor calibration is conducted on a database that consists of only 10 experimental results. In the second iteration, the database is expanded to a total of 11 results by adding a single FEA result to the 10 experimental results. The value of V_{FEA} used in Equation 11 to calculate k_i was 0.0398 and the calibrated capacity factor was updated from 0.8169 to 0.8232. The size of the database increases by one in every iteration, as a new FEA beam datum is added. In every iteration, the capacity factor for SFRRAC under flexure is updated. The purpose of this iterative procedure is to find the size of the database large enough to attain convergence of the calibrated capacity factor value. The following condition is used as the stopping criterion of the iterative procedure:

$$\left|\frac{\overline{b}_n - \overline{b}_{n-1}}{\overline{b}_n}\right| < 0.001 \;\&\; \left|\frac{V_{\delta n} - V_{\delta n-1}}{V_{\delta n}}\right| < 0.001 \quad (12)$$

where $\overline{b}_n$ and $\overline{b}_{n-1}$ are the bias correction factors when the size of the database is n and $n-1$, respectively; $V_{\delta n}$ and $V_{\delta n-1}$ are the modelling errors of the theoretical prediction method when the size of the database is n and $n-1$, respectively.

The c.o.v. of the modelling error of the theoretical capacity prediction method (V_δ) varies with respect to the size of the database. When the database consisted of only the 10 experimental data inputs, the value of V_δ was 0.0539. With the addition of FEA data, the value of V_δ decreased to 0.0399 when n was 28 and then started to fluctuate, as shown in Figure 4. However, the fluctuation in V_δ is not significant as it converges to 0.0419 when n is 83. With the increase in n, $\frac{\overline{b}_n - \overline{b}_{n-1}}{\overline{b}_n}$ decreases as shown in Figure 5. When n is 10, $\left|\frac{\overline{b}_n - \overline{b}_{n-1}}{\overline{b}_n}\right|$ is 0.0328, and it rapidly decreases to the value less than 0.005 by adding two FEA results. It finally converges to 0.0006 when n is 83.

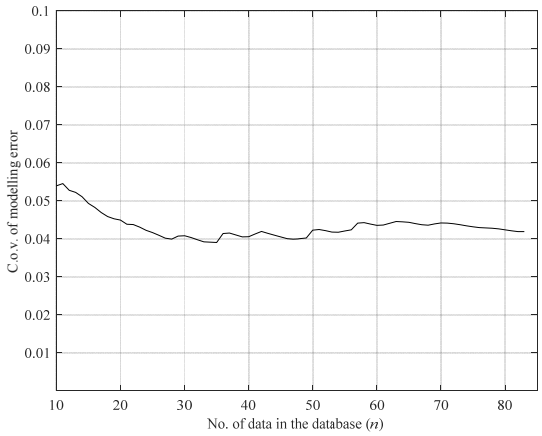

Figure 4: C.o.v. of modelling error vs. number of data

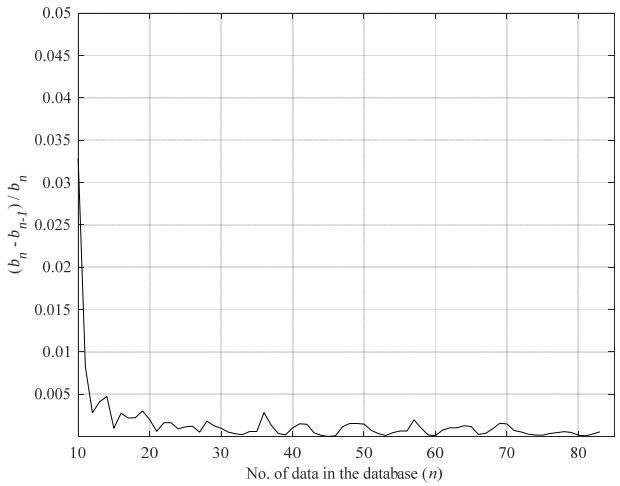

Figure 5: Convergence of bias correction factor with the number of data

4.1.2.3 Capacity factor for SFRRAC under flexure

Initially, when the database was only comprised of the 10 experimental data, the value of the calibrated capacity factor was 0.8169. On expanding the database by adding the FEA beam data, this value kept increasing until the size of the database was 33, and the value became 0.8436, which corresponds to the peak of the convergence plot denoted by the solid line in Figure 6. When more FEA data was added to further increase the size of the database, the value started decreasing slightly. Using the convergence criterion explained in Equation 12, the iteration stopped when the size of data was 83 and the value of the capacity factor for SFRRAC under flexure was 0.8305. Further expansion of the database will increase the computational cost of the capacity factor calibration without significantly changing the value of the capacity factor calibrated.

The solid line in Figure 6 represents the convergence of capacity factor when the target reliability index of 3.04 is used. Additionally, the capacity factor calibration was repeated for two other safety classes suggested in ISO 2394 (International Organization for Standardization, 1998). The values of the combined target reliability index for these classes are 3.1 and 4.3. The corresponding values of target reliability index for resistance alone are 0.8×3.1 = 2.48 and 0.8×4.3 = 3.44, respectively. The dashed and the dashed-dotted lines in Figure 6 show the convergence of the capacity factor when the target reliability index for resistance is 2.48 and 3.44, respectively.

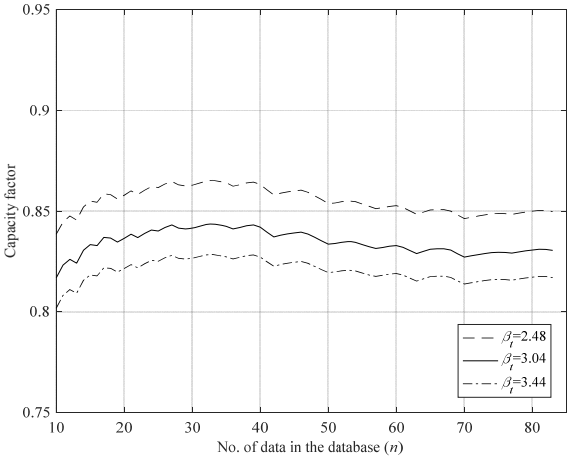

Figure 6: Convergence of capacity factor vs. number of data for different target reliability indices

The three plots in Figure 6 show that the convergence of capacity factor for SFRRAC under flexure does not depend on the target reliability index used in the reliability analysis. However, for a particular size of database, the value of capacity factor decreases, with the increase in the reliability index. When a database of 10 experimental data was used in the calibration procedure, the values of the calibrated capacity factors were 0.8385 and 0.8018 when the target reliability indices were 2.48 and 3.44, respectively. On increasing the size of the database, these calibrated capacity factor values converged to 0.8653 and 0.8285, respectively.

With the increase in the number of data, the corresponding value of the design fractile factor (k_d) would decrease and converge to a value of the target reliability index 3.04 for a large number of data, the c.o.v. of the modelling error of the capacity prediction method (V_δ) would converge to a particular value, the c.o.v. of the parametric uncertainty (V_{rt}) would remain the same and the fractile factor for FEA (k_{dFEA})

would converge for a large number of data. This is generic to all similar capacity factor calibration problems, if the data obtained from analytical models and numerical models have no significant error.

5. CONCLUSIONS

In this study, a proposed prediction model was developed to statistically and probabilistically predict the design moment-capacity of SFRRAC beams including the tensile contribution of SF unlike the conventional prediction model for NAC. This modification improved the accuracy of the prediction. FEA of SFRRAC was carried out. A parametric analysis was conducted by changing the dimensions of the SFRRAC beams. The results of FEA were compared with the experimental results to validate the accuracy of the FEA.

A design model for SFRRAC beams under flexure were developed in this study, in which capacity factor was calibrated using a proposed calibration procedure that can use both experimental and FEA data. This procedure considers the error due to the limited number of experimental data used to validate the accuracy of the numerical analysis, unlike previous studies. The capacity factor calibration was carried out on both existing SFRRAC beam test data from the literature, and new SFRRAC experimental data and the FEA data. The capacity factor for SFRRAC under flexure converges to a particular value when more data is added. The convergence of the capacity factor was checked using a stopping criterion. The stopping criterion was met when the size of the database was 83, showing that addition of more data will not significantly change the value of the calibrated capacity factor.

In future research, investigations on the performance of SFRRAC under other failure modes such as compression, shear and torsion can be studied in the future. Moreover, design models for the serviceability limit states of SFRRAC beam cross-sections can also be developed.

6. REFERENCES

ACI (American Concrete Institute). (2011). ACI 318-11: Building Code Requirements for Structural Concrete and Commentary. American Concrete Institute, Farmington Hills, MI, USA.

Bandyopadhyay, J. N. (2008). “Design of concrete structures.” Prentice Hall of India Learning Pvt. Ltd., New Delhi, India.

BSI (British Standards Institution). (2002). BS EN 1992:2002: Eurocode 0: Basis of structural design. BSI, London, UK.

BSI (British Standards Institution). (2004). BS EN 1992-1-1:2004: Eurocode 2: Design of concrete structures, Part 1-1: General rules and rules for buildings. BSI, London, UK.

International Organization for Standardization. (1998). ISO 2394-1998: General principles on reliability for structures, Geneva, Switzerland.

JCSS (Joint Committee on Structural Safety). (2001). JCSS Probabilistic model code Part 3 Material Properties, Joint Committee on Structural Safety.

Johnson, R. P., & Huang, D. (1994). “Calibration of safety factors γ_M for composite steel and concrete beams in bending.” Proceedings of the Institution of Civil Engineers - Structures and Buildings, *104*, 193-203.

Ravindrarajah, R. S. (1996). “Effects of Using Recycled Concrete as Aggregate on the Engineering Properties of Concrete.” Paper presented at National Symposium on the Use of Recycled Materials in Engineering Construction, Sydney, N.S.W, Australia.

Salman, M. M., and Abdul-Ameer, J. S. (2018). “Effect of recycled aggregates and steel fibers on flexural and shear behavior of reinforced normal concrete beams.” *Journal of Engineering and Sustainable Development*, *20*(1), 178-193.

Schubert, S., Hoffmann, C., Leemann, A., Moser, K., and Motavalli, M. (2012). “Recycled aggregate concrete: Experimental shear resistance of slabs without shear reinforcement.” *Engineering Structures*, *41*, 490-497.

Standards Australia. (2009). *Concrete structures* (AS 3600:2009). Homebush, NSW: Standards Australia.

Zhang, H. L., and Pei, C. C. (2017). “Flexural properties of steel fiber types and reinforcement ratio for high-strength recycled concrete beams.” *Advances in Structural Engineering*, *20*(10), 1512-1522.